https://doi.org/10.5607/en24004
Exp Neurobiol. 2024 Aug;33(4):202-214.
pISSN 1226-2560 • eISSN 2093-8144

Original Article

Experimental Neurobiology

Phosphorylated Tau in the Taste Buds of Alzheimer's Disease Mouse Models

Hyun Ji Kim[1,2†], Bo Hye Kim[3†], Dong Kyu Kim[3,4], Hanbin Kim[3,5], Sang-Hyun Choi[2], Dong-Hoon Kim[1,2], Myunghwan Choi[6], Inhee Mook-Jung[3,4,5], Yong Taek Jeong[1,2*] and Obin Kwon[3,4,5,7*]

[1]BK21 Graduate Program, Department of Biomedical Sciences, Korea University College of Medicine, Seoul 02841, [2]Department of Pharmacology, Korea University College of Medicine, Seoul 02841, [3]Department of Biochemistry and Molecular Biology, Seoul National University College of Medicine, Seoul 03080, [4]Convergence Research Center for Dementia, Seoul National University Medical Research Center, Seoul 03080, [5]Department of Biomedical Sciences, Seoul National University College of Medicine, Seoul 03080, [6]School of Biological Sciences, Seoul National University, Seoul 08826, [7]Sensory Organ Research Institute, Seoul National University Medical Research Center, Seoul 03080, Korea

Numerous systemic diseases manifest with oral symptoms and signs. The molecular diagnosis of Alzheimer's disease (AD), the most prevalent neurodegenerative disease worldwide, currently relies on invasive or expensive methods, emphasizing the imperative for easily accessible biomarkers. In this study, we explored the expression patterns of key proteins implicated in AD pathophysiology within the taste buds of mice. We detected the expression of amyloid precursor protein (APP) and tau protein in the taste buds of normal C57BL/6 mice. Phosphorylated tau was predominantly found in type II and III taste cells, while APP was located in type I taste cells. Remarkably, we observed significantly stronger immunoreactivity to phosphorylated tau in the taste buds of aged AD mouse models compared to age-matched controls. These findings underscore the oral expression of biomarkers associated with AD, highlighting the diagnostic potential of the oral cavity for neurodegenerative diseases.

Key words: Taste buds, Alzheimer's disease, Tauopathies, Amyloid protein precursor, Immunohistochemistry

INTRODUCTION

Many systemic diseases, including autoimmune, inflammatory, hematologic, and even endocrine disorders, can have oral manifestations [1]. While intraoral signs and symptoms alone may not confirm the presence of a disease, examination of any intraoral manifestations can be useful for assessing such conditions.

Taste buds are intraoral structures specialized for gustation [2]. Taste bud cells are referred to as neuroepithelial cells because, although they are derived from epithelium [3], they function like sensory neurons [4]. Taste cells respond to exogenous chemicals or tastants, generate action potentials [5], and interact with the primary neurons that innervate them by releasing neurotransmitter molecules at synapse-like structures [6]. Moreover, denervation of taste buds causes them to recede [7, 8], suggesting that taste buds are closely associated with the nervous system.

Alzheimer's disease (AD), the most common neurodegenerative disease, is characterized primarily by irreversible cognitive impairments, but it is also associated with changes in appetite. It remains unclear whether these changes in appetite stem from peripheral taste bud defects or central cognitive impairments that interfere with the processing of taste information. Recently, several animal studies using genetic models for AD have examined the effects of AD on the structure of taste buds and on gustatory function [9,

Submitted February 15, 2024, Revised July 5, 2024,
Accepted August 8, 2024

*To whom correspondence should be addressed.
Yong Taek Jeong, TEL: 82-2-2286-1295, FAX: 82-2-927-0824
e-mail: jyongtaek@korea.ac.kr
Obin Kwon, TEL: 82-2-740-8240, FAX: 82-2-3668-7897
e-mail: obinkwon@snu.ac.kr
†These authors contributed equally to this article.

10]. To date, however, no study has investigated the diagnostic potential of taste buds in relation to AD, such as taste bud expression of AD biomarkers.

Because AD is already irreversible when diagnosed clinically, many groups are working to develop methods of earlier diagnosis. AD is characterized by the deposition of extracellular amyloid plaques and intracellular neurofibrillary tangles (NFTs) in the brain. In the amyloidogenic pathway, amyloid precursor protein (APP) is serially cleaved by β- and γ-secretases on the plasma membrane, releasing toxic amyloid beta (Aβ) isoforms [11]. Among these, the hydrophobic and insoluble $A\beta_{42}$ isoform is particularly neurotoxic. Tau protein normally stabilizes microtubules in neuronal axons, while NFTs are protein aggregates composed of phosphorylated tau (p-tau). Aβ- and tau-related molecules serve as core AD biomarkers, but the current molecular diagnosis of AD using these biomarkers is invasive (requiring lumbar puncture) and/or expensive (imaging studies) [11]. Thus, approaches that rely on current biomarkers are insufficient for AD screening or follow-up. The development of novel diagnostic methods that are more cost-effective and non-invasive is critical.

In addition to their expression in the brain, the core AD biomarkers are also found in the periphery [12]. In this study, we report the expression of APP and tau in taste buds of normal mice in a cell type-specific manner and the detection of p-tau in taste buds of aged AD mouse models.

MATERIALS AND METHODS

Mice

Animals were treated and maintained under the approval of and in accordance with the standards of the Institutional Animal Care and Use Committee of Seoul National University (SNU-200704-2). C57BL/6 mice were purchased from KOATECH (Korea). Three ADLP mouse models were used in this study. $ADLP^{APP/PS1}$ mice (5xFAD mice, JAX #006554); $ADLP^{Tau}$ mice (TauP301L-JNPL3 homozygote; Taconic #2508) backcrossed with B6SJL (C57BL/6 X SJL); $ADLP^{APT}$ mice that were produced by crossing $ADLP^{APP/PS1}$ mice and $ADLP^{Tau}$ mice [13]. All the ADLP mice used for IHC experiments in this study were 14~16-month-old females. The mice were housed at a controlled temperature under a 12-hour light-dark cycle with free access to a standard chow and water.

Immunohistochemistry (IHC)

Mice were perfused with 0.1 M phosphate-buffered saline (PBS). Harvested tongues were post-fixed with 4% paraformaldehyde in PBS, dehydrated in 30% sucrose in PBS, and embedded in Tissue-Tek OCT compound (Sakura Finetek, Japan). Samples were coronally cut into at 14 μm. For FuP, free-floating sections were collected. For foliate papillae (FoP) and circumvallate papilla (CVP), the tissue sections were mounted directly onto slide glass. All the sections were blocked in 5% goat serum or donkey serum in PBS containing 0.3% Triton X-100 (PBST). Samples were incubated in primary antibodies diluted in blocking buffer. In next day, the samples were incubated with secondary antibodies in PBST for 2 hours at room temperature. DAPI (1:5,000; D9542, Sigma) staining was performed after washes. Free-floated fungiform papillae (FuP) sections were mounted on slide glass after staining. All the samples were covered with Vectashield (Vector Laboratories, CA) and a cover glass. Antibodies information is available in Table 1. Images were acquired with an LSM800 confocal microscope (Zeiss, Germany).

Immunofluorescent (IF) signal quantification

For APP, tau and p-tau staining, all the samples for AD mouse models were stained simultaneously under identical conditions and their IF signals were acquired with identical microscope settings to facilitate comparisons. Taste buds and surrounding epithelial cells were distinguished based on the shape and alignment direction of DAPI-stained nuclei. Cell type-specific expression of AD biomarkers was assessed by their co-localization with Trpm5 or Car4 signals or their circumscription by NTPDase2 signals. Based on this criterion, we established the region of interest for subsequent quantitative measurement of the IF intensity using Image J software.

Statistical analyses

Data in graphs were presented as violin plots with raw values. Statistical differences between groups were analyzed using one-way analysis of variance (ANOVA) with Bonferroni's multiple comparisons for post-hoc analysis or Kruskal Wallis test with Dunn-Bonferroni correction for post-hoc analysis.

RESULTS

APP and p-tau proteins are expressed in taste buds

Considering that the core biomarkers of AD, APP and tau protein, are primarily produced by neurons, and that taste buds contain cells that exhibit neuron-like features, we asked whether APP and tau are expressed in taste buds. Using an antibody against APP (6E10) in 8-week-old C57BL/6 mice, we performed an IHC experiment and found immunoreactivity (IR) in the taste buds of FuP (Fig. 1A′), FoP (Fig. 1A″), and CVP (Fig. 1A‴). Similarly, using an antibody against tau (Tau13), we found IR in the taste buds of FuP (Fig. 1B′), FoP (Fig. 1B″), and CVP (Fig. 1B‴). As most mouse-

Table 1. Primary and secondary antibodies used in this study

Target	Source	Cat#	Dilution
Primary antibodies			
Biotin-labeled 6E10	BioLegend	#803007	1:200
Tau13	Abcam	ab19030	1:200
AT8, Ser202/Thr205	Thermo fisher Scientific	MN1020	1:200
AT180, Thr231/Ser235	Thermo fisher Scientific	MN1040	1:200
Anti-NTPDase II	CHUQ	mN2-36LI6	1:1,000
Anti-Trpm5	In house	N/A	1:500
Anti-Car4	R&D Systems	AF2414	1:1,000
Secondary antibodies			
Goat anti-Rabbit IgG (H+L) Highly Cross-Adsorbed Secondary Antibody, Alexa Fluor™ Plus 488	Thermo fisher Scientific	A32731	1:1,000
Goat anti-Guinea Pig IgG (H+L) Highly Cross-Adsorbed Secondary Antibody, Alexa Fluor™ 488	Thermo fisher Scientific	A11073	1:1,000
Goat anti-Mouse IgG (H+L) Highly Cross-Adsorbed Secondary Antibody, Alexa Fluor™ Plus 555	Thermo fisher Scientific	A32727	1:1,000
Goat anti-Rabbit IgG (Heavy chain), Superclonal™ Recombinant Secondary Antibody, Alexa Fluor™ 647	Thermo fisher Scientific	A27040	1:1,000
Donkey anti-Mouse IgG (H+L) Highly Cross-Adsorbed Secondary Antibody, Alexa Fluor™ 488	Thermo fisher Scientific	A21202	1:1,000
Donkey anti-Goat IgG (H+L) Highly Cross-Adsorbed Secondary Antibody, Alexa Fluor™ Plus 555	Thermo fisher Scientific	A32816	1:1,000

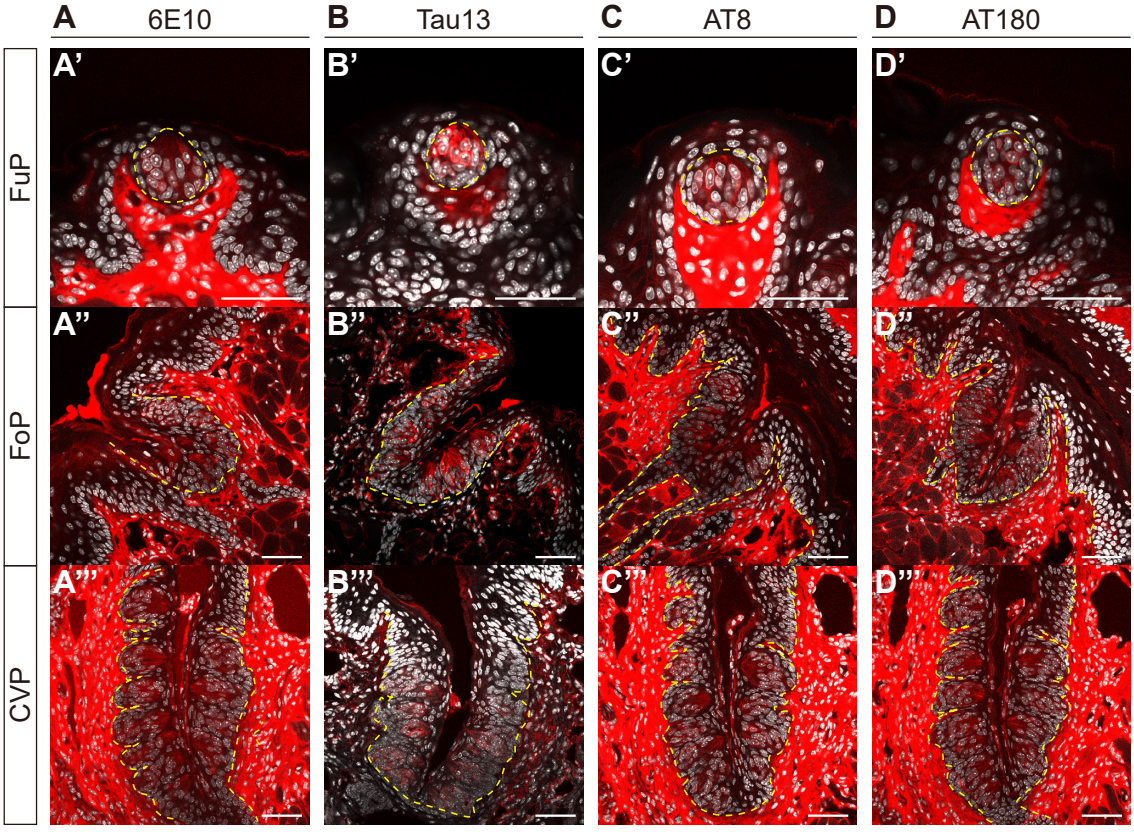

Fig. 1. Detection of amyloid precursor protein (APP) and phosphorylated tau (p-tau) in taste buds. Representative confocal images of 6E10-immunoreactivity (IR) (A), Tau13-IR (B), AT8-IR (C), and AT180-IR (D) in fungiform (FuP) (A′~D′), folate (FoP) (A″~D″), and circumvallate papillae (CVP) (A‴~D‴) of 8-week-old C57BL/6 mice. Yellow dashed lines demarcate the epithelial boundaries. Immunofluorescent (IF) signals (red) and DAPI (white). Scale bars=50 μm.

https://doi.org/10.5607/en24004

derived monoclonal antibodies induce autofluorescence in lingual stromal areas but not in the epithelial layers (data not shown), this study only accounts for epithelial IR. Additionally, it is important to mention that the 6E10 antibody does not distinguish APP from $A\beta_{1-16}$ [14]. Given that the positive signals were detected in intracellular parts, we considered that they might be derived from APP rather $A\beta_{1-16}$.

As tau phosphorylation is widely regarded as a pathological hallmark of AD brains, we next asked whether tau proteins in taste buds also undergo phosphorylation. In 8-week-old C57BL/6 mice, we conducted an IHC using two independent antibodies, AT8 (pS202/T205) and AT180 (pT231/S235). These antibodies specifically recognize p-tau associated with the pre-tangle stage of AD progression [15, 16] and offer the advantage of specificity, as they do not cross-react with unphosphorylated forms of tau [17, 18]. Similar to Tau13-IR, we also detected AT8-IR and AT180-IR in the intragemmal cells of FuP (Fig. 1C′, D′), FoP (Fig. 1C″, D″), and CVP (Fig. 1C‴, D‴). These data confirm that intragemmal tau proteins can be phosphorylated, which may implicate them in AD pathology.

Cell-type specific expression of APP and p-tau in taste buds

To identify the cell types that express APP and/or p-tau in taste buds, we conducted a double IHC using 6E10 or AT180 with several intragemmal cell markers: NTPdase2 for type I taste cells; Trpm5 for type II taste cells; and Car4 for type III taste cells. We found 6E10-IR in type I taste cells (Fig. 2A), and around two-thirds of the type II taste cells (Fig. 2B), but not in type III taste cells (Fig. 2C). This cell type specificity did not depend on papilla type. Meanwhile, for p-tau, we observed AT180-IR in both type II (Fig. 2E′) and type III taste cells (Fig. 2F′) in FuP, but not in type I taste cells (Fig. 2D′). In CVP, we detected AT180-IR only in type II taste cells (Fig. 2E″). These data indicate that the AD-related proteins are expressed in a cell-type specific manner in taste buds.

Phosphorylated-tau is highly expressed in the taste buds of AD mouse models

Considering their expression in taste buds, we next asked whether APP and p-tau expression are elevated in mouse models of AD-like pathology (ADLP). We evaluated 14~16-month-old $ADLP^{APP/PS1}$ (amyloidopathy model), $ADLP^{Tau}$ (tauopathy model), and $ADLP^{APT}$ (combined amyloidopathy and tauopathy model) mice with age-matched littermate controls [13]. Using the same image acquisition settings, we found increased AT8-IR and AT180-IR in the CVP of all AD mouse models with tauopathy ($ADLP^{Tau}$ and $ADLP^{APT}$) compared to controls (Fig. 3, Table 2, 3). $ADLP^{APT}$ mice showed higher AT8-IR and AT180-IR compared to $ADLP^{Tau}$. Compared to CVP, the overall intergroup difference in FuP was blunted (Fig. 4, Table 4, 5), which may be due to the relatively small number of taste buds. Nevertheless, similar increase in AT8-IR was prominent in the FuP of all AD mouse models compared to controls. In both CVP and FuP, $ADLP^{APT}$ showed higher AT8-IR compared to all the other groups, while their intergroup difference in AT180-IR or 6E10 was relatively blunted. Interestingly, intragemmal cells of $ADLP^{APP/PS1}$ mice exhibited no increase in 6E10-IR compared to those of controls, suggesting that the differential expression of these markers in taste buds reflects AD-like features rather than merely originating from genetic manipulation.

Taste tissues in AD mouse models show intact histologic architecture

To determine whether APP and p-tau in intragemmal cells affect the histological integrity of taste cells in AD mouse models, we performed an IHC with taste cell type-specific markers (Fig. 5). We found similar numbers of taste buds and similar taste cell composition in AD mouse models compared to age-matched control mice (Fig. 5A-D). This suggests that although we did detect AD-related markers in the taste buds of the AD models, taste bud architecture remained intact.

DISCUSSION

This study aimed to investigate the detection of core AD biomarkers in taste buds, which are neuroepithelial cells outside the brain. We discovered cell-type specific expression of APP, tau protein, and p-tau protein in taste buds. When we examined the expression of APP and p-tau in AD mouse models, we found their taste cells showed stronger expression than age-matched controls. This study represents the first report of APP and tau protein expression in the taste buds.

Although APP and tau protein have been primarily studied in AD brain tissues, there is evidence for their peripheral expression outside the brain [12, 19, 20]. According to the Human Protein Atlas (proteinatlas.org; accessed in November 2023) [21], microtubule associated protein tau (*MAPT*) transcripts are expressed at higher levels in the human tongue than any other peripheral organ except skeletal muscle. Interestingly, APP expression levels in the tongue are moderate. In mice, *App* RNA is weakly detectable on embryonic day 14.5 using *in situ* hybridization, as reported by the Mouse Genome Database at Mouse Genome Informatics (www.informatics.jax.org; accessed in November 2023) [22]. The spatial distribution of APP's expression, however, does not align with the location of taste buds. Currently, there are no available data for the expression of *Mapt* RNA in mouse tongue. To the best of our

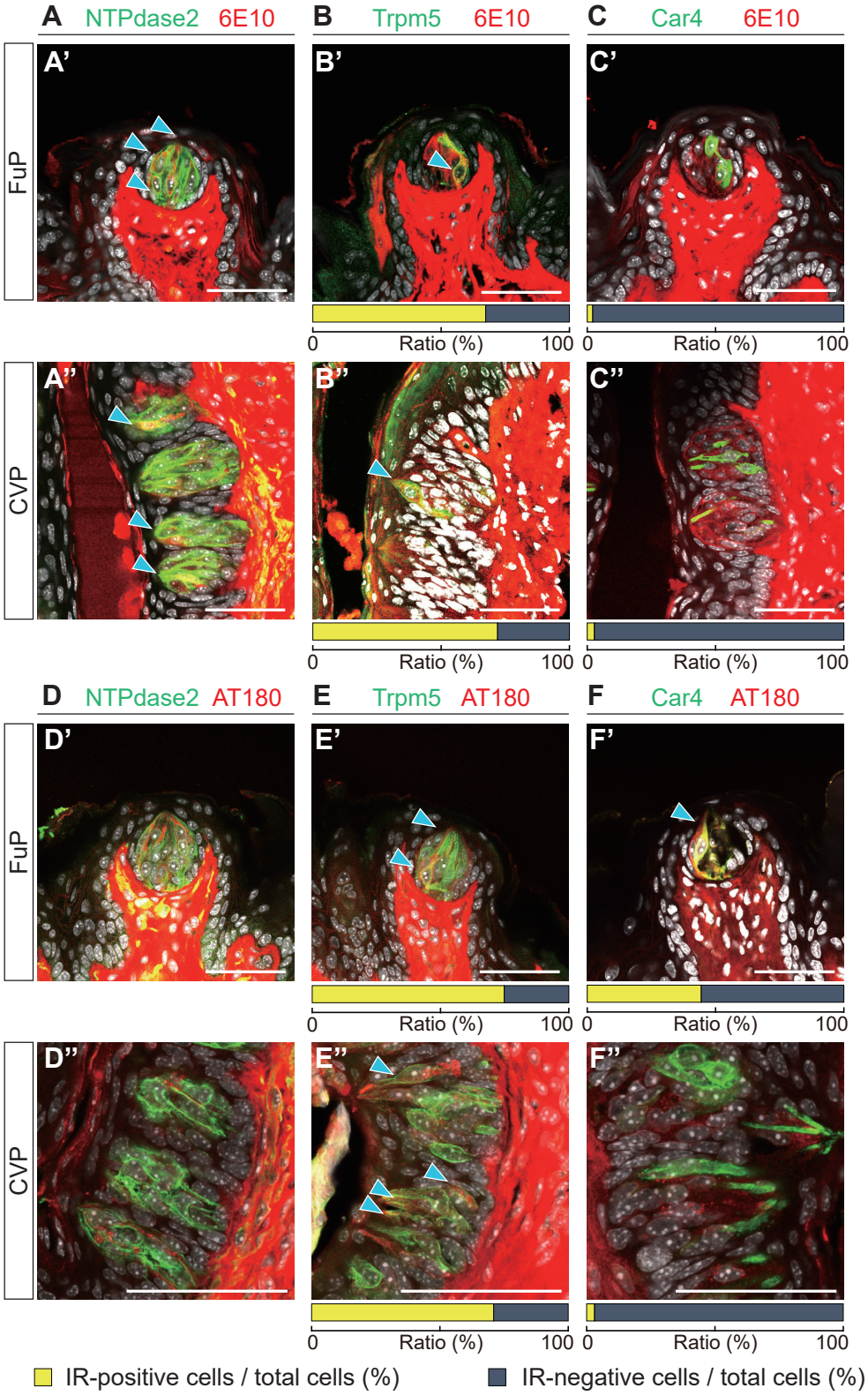

Fig. 2. Localization of APP and p-tau in taste cells. (A~C) Double fluorescent images of FuP (A′~C′) and CVP (A″~C″) showing 6E10-IR (red) with cell-type specific markers (green). (D~F) Double fluorescent images of FuP (D′~F′) and CVP (D″~F″) showing AT180-IR (red) with cell-type specific markers (green). Anti- NTPdase2 for type I cells (A, D), anti-Trpm5 for type II cells (B, E), or anti-Car4 for type III cells (C, F). Blue arrowheads indicate colocalization. Scale bars=50 μm. Ratio of IR-positive (yellow bars) and IR-negative cells (gray bars) among type II and type III taste cells were indicated under the tissue images.

https://doi.org/10.5607/en24004

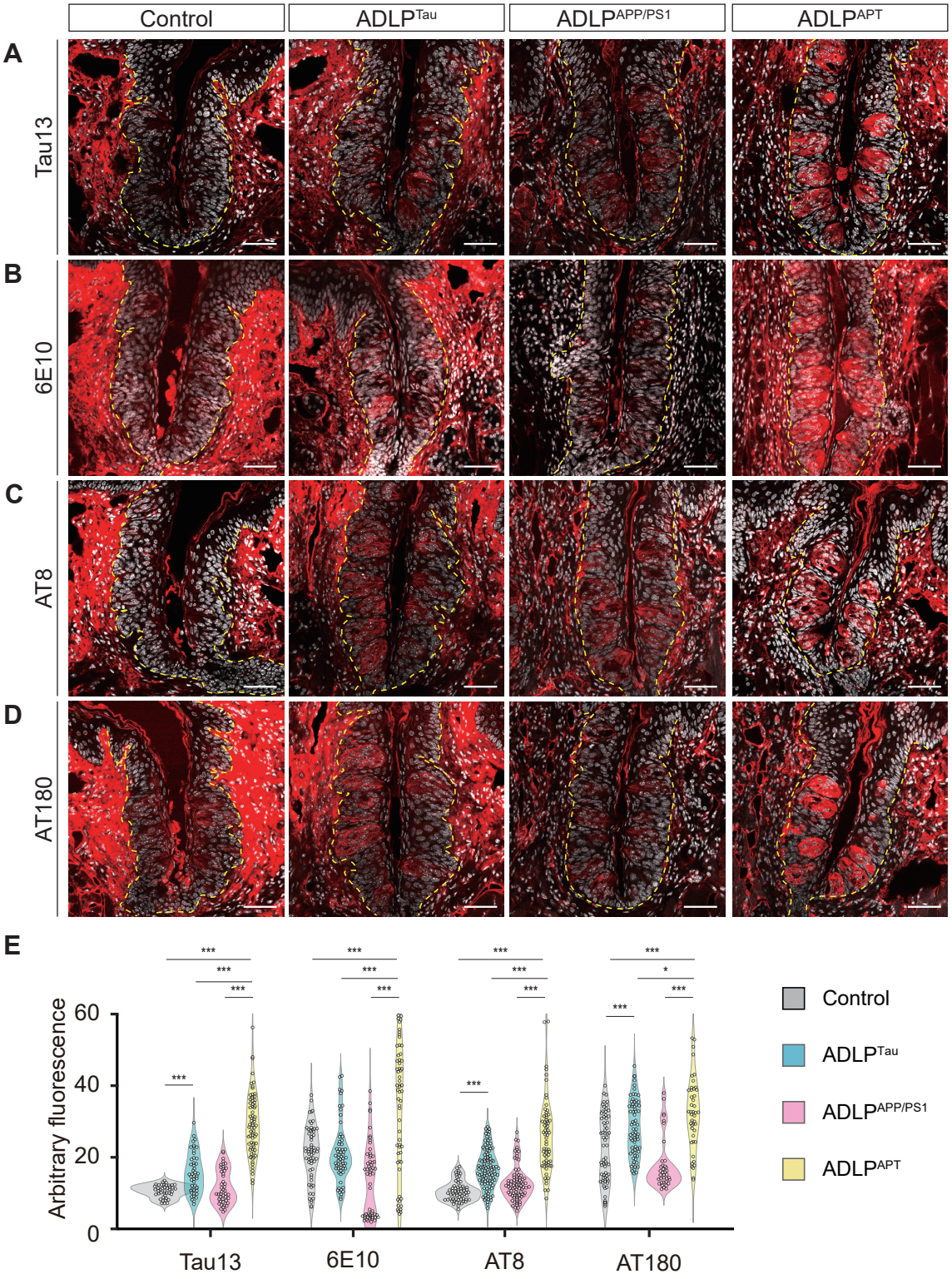

Fig. 3. Comparison of APP and p-tau in CVP of Alzheimer's disease (AD) mouse models. Representative images of Tau13-IR (A), 6E10-IR (B), AT8-IR (C), and AT180-IR (D) in control, ADLP^{Tau}, ADLP$^{APP/PS1}$, and ADLP^{APT} mice. Yellow dashed lines demarcate the outer boundaries of taste buds. IF signals (red) and DAPI (white). Scale bars=50 μm. (E) Intensity quantification for Tau13-IR, 6E10-IR, AT8-IR, and AT180-IR in AD mouse models. *p<0.05, ***p<0.005. Detailed statistical information is available in Tables 2, 3.

Table 2. The information for descriptive statistics corresponding to Fig. 3

Antibody	Genotype	Numbers		Mean	Std. Dev.	Std. Error
		Mice	Taste buds			
Tau13	Control	3	42	10.4064	1.7369	0.2680
	$ADLP^{Tau}$		46	15.5456	5.6016	0.8259
	$ADLP^{APP/PS1}$		46	11.5615	4.7526	0.7007
	$ADLP^{APT}$		72	29.0075	8.5009	1.0018
6E10	Control	3	63	20.9688	7.5910	0.9564
	$ADLP^{Tau}$		60	21.0004	8.2966	1.0711
	$ADLP^{APP/PS1}$		58	13.2007	9.9949	1.3124
	$ADLP^{APT}$		65	35.8945	18.4041	2.2827
AT8	Control	4	63	10.3767	2.7882	0.3513
	$ADLP^{Tau}$		106	16.6794	5.3498	0.5196
	$ADLP^{APP/PS1}$		82	12.5419	4.7330	0.5227
	$ADLP^{APT}$		66	25.7645	10.0019	1.2311
AT180	Control	3	67	21.7462	9.5964	1.1724
	$ADLP^{Tau}$		69	28.0023	7.7643	0.9347
	$ADLP^{APP/PS1}$		37	17.7461	7.2977	1.1997
	$ADLP^{APT}$		46	32.5635	10.8534	1.6002

Table 3. The information for inferential statistics corresponding to Fig. 3. To test for statistical significance, one-way ANOVA with Bonferroni post-hoc analysis was used for the fluorescent intensity values

Antibody	One-way ANOVA			Groups tested	Bonferroni's multiple comparison
	df	F value	p value		p-value
Tau13	3	116.645193	<0.0001	Control vs $ADLP^{Tau}$	0.0008
				Control vs $ADLP^{APP/PS1}$	1.000
				Control vs $ADLP^{APT}$	<0.0001
				$ADLP^{Tau}$ vs $ADLP^{APP/PS1}$	0.0133
				$ADLP^{Tau}$ vs $ADLP^{APT}$	<0.0001
				$ADLP^{APP/PS1}$ vs $ADLP^{APT}$	<0.0001
6E10	3	38.886514	<0.0001	Control vs $ADLP^{Tau}$	1.0000
				Control vs $ADLP^{APP/PS1}$	0.0028
				Control vs $ADLP^{APT}$	<0.0001
				$ADLP^{Tau}$ vs $ADLP^{APP/PS1}$	0.0031
				$ADLP^{Tau}$ vs $ADLP^{APT}$	<0.0001
				$ADLP^{APP/PS1}$ vs $ADLP^{APT}$	<0.0001
AT8	3	82.156094	<0.0001	Control vs $ADLP^{Tau}$	<0.0001
				Control vs $ADLP^{APP/PS1}$	0.2168
				Control vs $ADLP^{APT}$	<0.0001
				$ADLP^{Tau}$ vs $ADLP^{APP/PS1}$	<0.0001
				$ADLP^{Tau}$ vs $ADLP^{APT}$	<0.0001
				$ADLP^{APP/PS1}$ vs $ADLP^{APT}$	<0.0001
AT180	3	24.258543	<0.0001	Control vs $ADLP^{Tau}$	<0.0001
				Control vs $ADLP^{APP/PS1}$	0.1861
				Control vs $ADLP^{APT}$	<0.0001
				$ADLP^{Tau}$ vs $ADLP^{APP/PS1}$	<0.0001
				$ADLP^{Tau}$ vs $ADLP^{APT}$	0.0498
				$ADLP^{APP/PS1}$ vs $ADLP^{APT}$	<0.0001

knowledge, no studies have investigated tau expression in the taste buds of mice or humans.

Under physiological conditions, the positively charged tau protein plays a crucial role in stabilizing neuronal microtubules, which are negatively charged. During AD pathogenesis, however, tau undergoes hyperphosphorylation, reducing its charge and causing detachment from microtubules [23], typically triggering the onset of tauopathy. There are far fewer studies investigating p-tau in non-neuronal cells of organs outside the brain than studies in the brain. Two potential mechanisms can explain the appearance of p-tau in peripheral organs: either tau is phosphorylated directly in the periphery or p-tau is transmitted into the periphery along neurons from its origin in an aging brain. The former possibility aligns with the premise of the Braak hypothesis, which suggests periph-

https://doi.org/10.5607/en24004

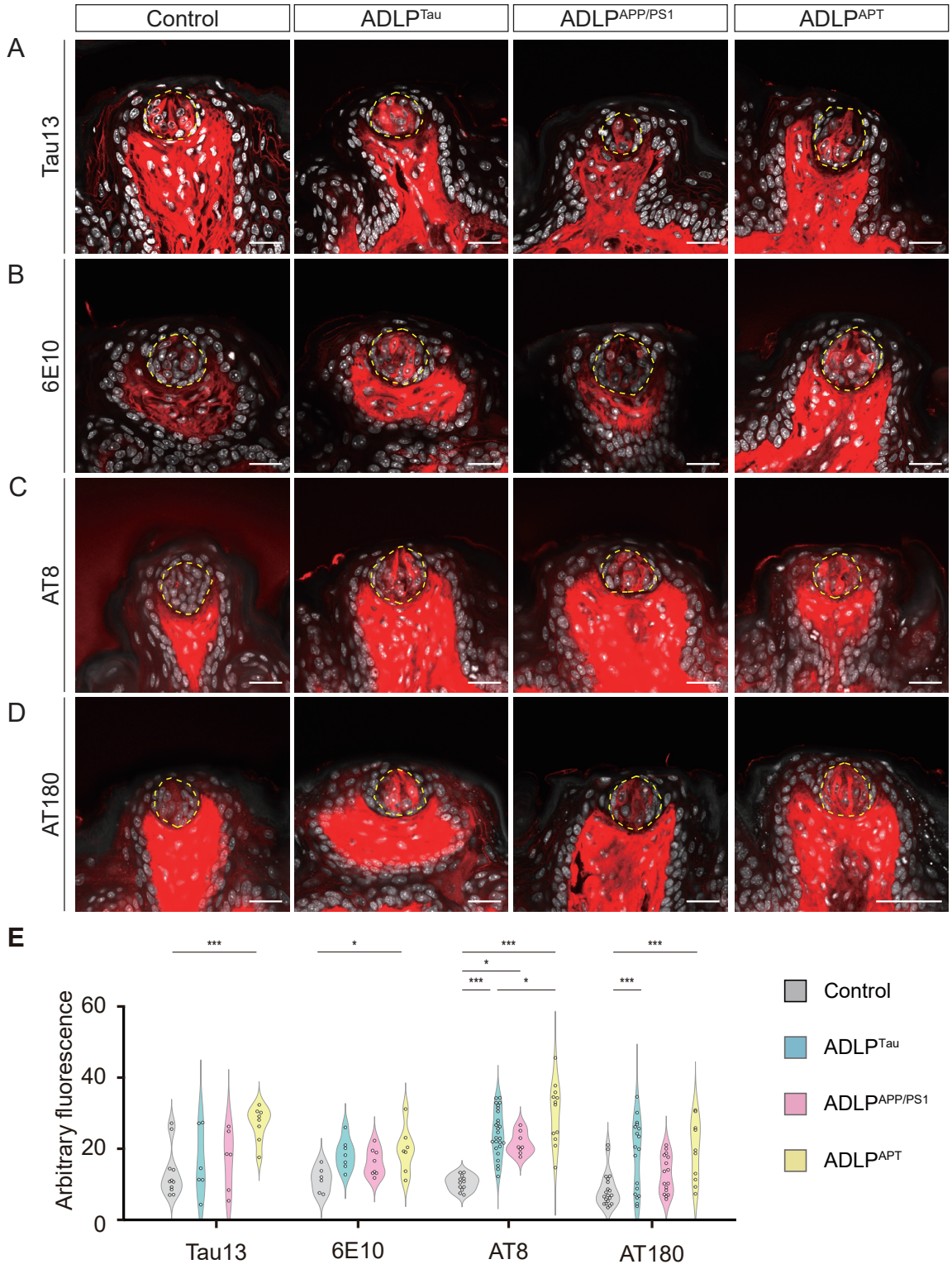

Fig. 4. Comparison of APP and p-tau in FuP of AD mouse models. Representative images of Tau13-IR (A), 6E10-IR (B), AT8-IR (C), and AT180-IR (D) in control, ADLP^{Tau}, ADLP$^{APP/PS1}$, and ADLP^{APT} mice. Yellow dashed lines demarcate the outer boundaries of taste buds. Immunofluorescent signals (red) and DAPI staining (white). Representative images were selected from 3~4 mice per group. Scale bars=50 μm. (E) Intensity quantification for Tau13-IR, 6E10-IR, AT8-IR, and AT180-IR in AD mouse models. *p<0.05, ***p<0.005. Detailed statistical information is available in Tables 4, 5.

Table 4. The information for descriptive statistics corresponding to Fig. 4

Antibody	Genotype	Numbers		Mean	Std. Dev.	Std. Error
		Mice	Taste buds			
Tau13	Control	3	11	13.5288	7.0815	2.1351
	$ADLP^{Tau}$		6	16.3333	9.5543	3.9005
	$ADLP^{APP/PS1}$		6	17.3395	8.6929	3.5489
	$ADLP^{APT}$		8	18.4625	9.1140	1.6370
6E10	Control	3	6	11.5759	3.6108	1.4741
	$ADLP^{Tau}$		7	18.8884	4.4876	1.6961
	$ADLP^{APP/PS1}$		8	16.4752	3.8757	1.3703
	$ADLP^{APT}$		7	20.1139	6.6599	2.5172
AT8	Control	4	12	10.6253	2.1794	0.6291
	$ADLP^{Tau}$		28	24.4197	6.7144	1.2689
	$ADLP^{APP/PS1}$		8	21.9760	3.1899	1.1278
	$ADLP^{APT}$		12	30.7265	8.8399	2.5519
AT180	Control	4	20	8.7167	5.0010	1.1183
	$ADLP^{Tau}$		19	18.8858	10.1192	2.3215
	$ADLP^{APP/PS1}$		16	13.0155	5.4016	1.3504
	$ADLP^{APT}$		12	20.6610	8.4420	2.4370

Table 5. The information for inferential statistics corresponding to Fig. 4. To test for statistical significance, Kruskal Wallis test by Dunn-Bonferroni correction was used for the fluorescent intensity values

Antibody	Kruskal-Wallis Test			Groups tested	Bonferroni's multiple comparison
	Test statistic	df	p value		p-value
Tau13	12.343	3	0.006	Control vs $ADLP^{Tau}$	1.000
				Control vs $ADLP^{APP/PS1}$	1.000
				Control vs $ADLP^{APT}$	0.004
				$ADLP^{Tau}$ vs $ADLP^{APP/PS1}$	1.000
				$ADLP^{Tau}$ vs $ADLP^{APT}$	0.1908
				$ADLP^{APP/PS1}$ vs $ADLP^{APT}$	0.1231
6E10	8.610	3	0.035	Control vs $ADLP^{Tau}$	0.0856
				Control vs $ADLP^{APP/PS1}$	0.5482
				Control vs $ADLP^{APT}$	0.0465
				$ADLP^{Tau}$ vs $ADLP^{APP/PS1}$	1.000
				$ADLP^{Tau}$ vs $ADLP^{APT}$	1.000
				$ADLP^{APP/PS1}$ vs $ADLP^{APT}$	1.000
AT8	32.529	3	<0.0001	Control vs $ADLP^{Tau}$	<0.0001
				Control vs $ADLP^{APP/PS1}$	0.0272
				Control vs $ADLP^{APT}$	<0.0001
				$ADLP^{Tau}$ vs $ADLP^{APP/PS1}$	1.000
				$ADLP^{Tau}$ vs $ADLP^{APT}$	0.0305
				$ADLP^{APP/PS1}$ vs $ADLP^{APT}$	0.2650
AT180	19.059	3	<0.0001	Control vs $ADLP^{Tau}$	0.0029
				Control vs $ADLP^{APP/PS1}$	0.3574
				Control vs $ADLP^{APT}$	0.0007
				$ADLP^{Tau}$ vs $ADLP^{APP/PS1}$	0.9241
				$ADLP^{Tau}$ vs $ADLP^{APT}$	1.000
				$ADLP^{APP/PS1}$ vs $ADLP^{APT}$	0.2611

eral-to-brain transmission based on the observation of p-tau in the olfactory structures of AD patients [24, 25]. The detection of p-tau in the taste buds of normal mice in this study also suggests endogenous tau protein in taste buds can be phosphorylated. Conversely, because type II and III taste cells are closely connected to primary gustatory neurons, it will be important to determine whether intragemmal p-tau is delivered to the brain where it could contribute to AD pathology.

The finding that p-tau and APP are expressed in taste buds in a cell type-specific manner was one of interesting findings of this study. We observed p-tau expression primarily in type II and III taste cells, which both harbor neuron-like features [7]. This is consistent with the typical expression of tau in neurons rather than astrocytes or microglia [26]. Although recent studies documented

https://doi.org/10.5607/en24004

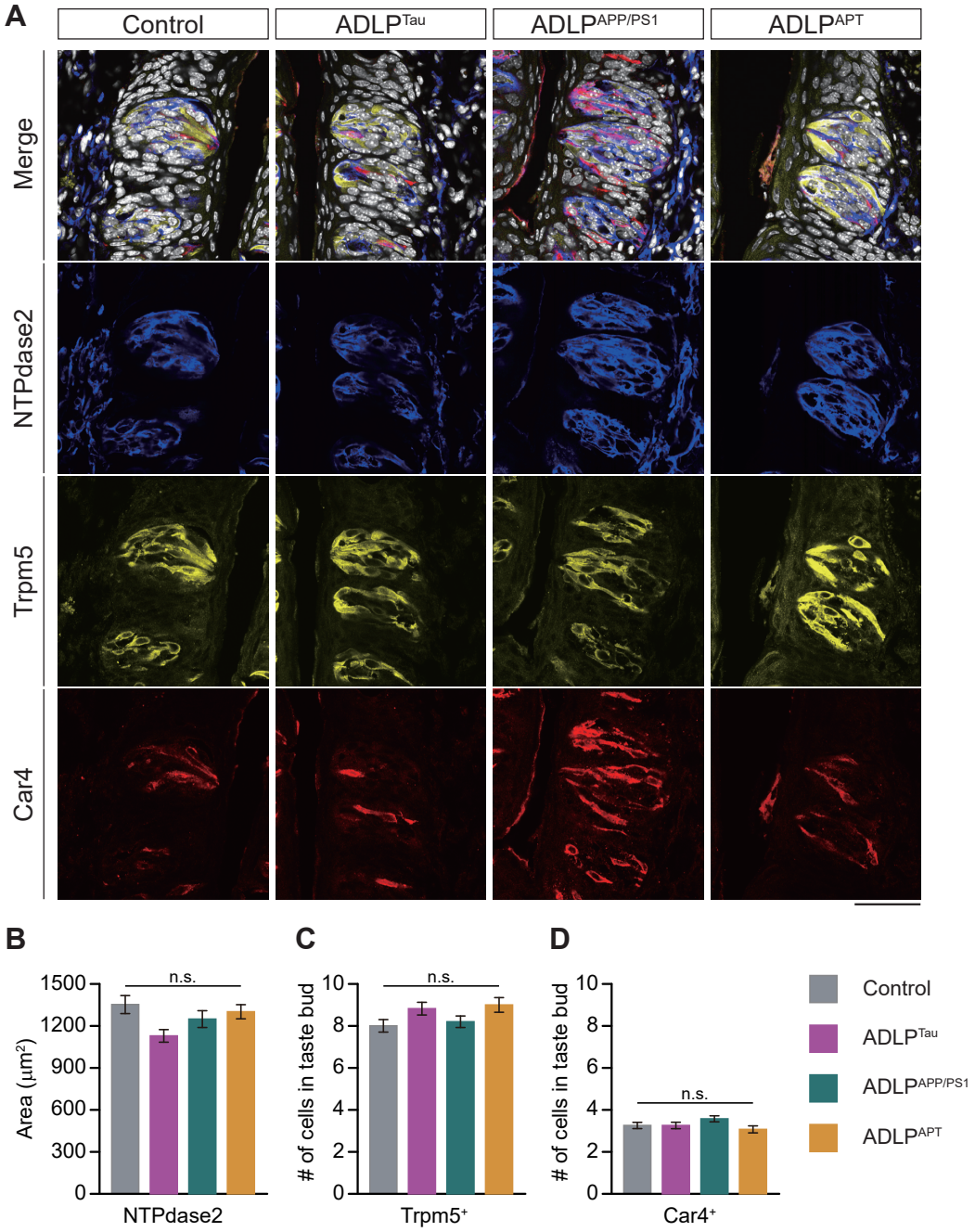

Fig. 5. Intact histologic architecture of the CVP in AD mouse models. (A) Representative merged and split confocal images showing the expression of cell-specific markers for type I taste cells: anti-NTPdase2 in blue, type II taste cells: anti-Trpm5 in yellow, and type III taste cells: anti-Car4 in red in AD mouse models. DAPI appears in white. Scale bars=50 μm. (B) The average size of areas occupied by anti-NTPdase2 immunosignals in taste buds. (C) The average number of Trpm5+ cells in a taste bud in AD mouse models. (D) The average number of Car4+ cells in a taste bud in AD mouse models. n.s. Not significant.

the transmission of tau pathology from neurons to glial cells such as astrocytes [27], taste cells are unlikely to experience enough tau aggregation to enable intercellular transmission due to their frequent turnover. We found expression of APP, however, in type I taste cells, which function similar to glial cells. Since APP expression in the brain is rich in neurons and peaks during synaptogenesis, it is difficult to interpret the expression of APP in taste buds. Future research on the gene expression profiling of each taste cell type using single cell sequencing methods may provide valuable insights into this phenomenon.

The increased expression of p-tau in the taste buds of various AD mouse models supports the potential utility of the oral mucosa as a biomarker for AD. Particularly noteworthy is the finding that ADLP^{APT} mice exhibited higher levels of AT8-IR and AT180-IR than ADLP^{Tau} mice, which is consistent with the previous report that ADLP^{APT} mice displayed more severe NFT pathology in the hippocampus than ADLP^{Tau} mice [13]. Interestingly, ADLP^{APT} mice also exhibited higher levels of 6E10-IR than any other group in CVP, although even ADLP$^{APP/PS1}$ mice showed no increase in 6E10-IR compared to control mice. This finding raises the question of whether p-tau can reciprocally increase APP, which needs further evaluation.

Recently, several groups investigated whether the appetite alterations of AD patients result from structural or functional changes in the gustatory system. Using different genetic AD models, two independent studies reported that the taste sensitivity of amyloidopathic mice was unaffected, even in late stages [9, 28]. This suggests AD appetite alterations may be due to defective taste information processing in the brain, rather than defective peripheral taste detection. Consistent with this, we were unable to observe any differences in the composition of mature intragemmal cells in either amyloidopathy or tauopathy mouse models. We propose two potential explanations for the preserved integrity of taste buds in AD mouse models. First, the average life span of a taste cell is very short, ranging from 3~21 days, whereas most brain neurons survive throughout the life of the organism [29, 30]. This suggests taste bud cells may be recycled before they succumb to tau aggregate-induced cytotoxicity. Alternatively, a lack of axon-like structures may dampen the toxic effects of tau aggregation in taste bud cells because tau aggregate-induced neurotoxicity arises mainly from the disassembly of axonal microtubules.

Through this work, intraoral specimens have emerged as promising options for AD diagnosis because they are non-invasive and cost-effective. Salivary $A\beta_{42}$ and p-tau have been proposed as diagnostic indicators for AD, but currently, the correlations between salivary biomarkers and the various stages of AD progression, as identified through cerebrospinal fluid (CSF) analysis or brain imaging, still seem controversial [31-36]. Indeed, oral epithelial cells have also been suggested as specimens for AD diagnosis. Tau expression was higher in the exfoliated oral epithelial cells of AD patients than in patients with vascular dementia or in healthy controls [37]. Moreover, the authors of that study also suggested a positive correlation between tau levels in the oral epithelium and CSF. Another study demonstrated an increased proportion of oral mucosal cells expressing p-tau (pS202) in patients with severe cognitive impairment compared to those with mild cognitive impairment and controls [38]. But these cells are unlikely to share neuron-like features. We therefore hope that taste cells, we suggest, will be more compatible and relevant peripheral specimens for AD diagnosis and prognosis.

We acknowledge several limitations of this study. First, this study only presents the expression of APP and p-tau in the taste buds of mice at a specific age; an investigation of the age-dependent expression may provide further insights. Second, we utilized AD mouse models that replicate familial AD in humans. Since the majority of AD cases are sporadic, it is important to determine whether higher p-tau levels can be detected in the taste buds of AD animal models that mimic sporadic AD in humans [39]. Furthermore, a study of postmortem or fresh human taste buds may be required to uncover any correlation between p-tau expression and disease severity. Last, clinical measurements of p-tau levels in taste buds may require the development of novel, non-invasive techniques. Considering the superficial location of taste buds, fluorescent probes for imaging p-tau can be tested [40].

In conclusion, our study provides evidence of the presence of AD biomarkers, particularly p-tau, in the taste buds of AD model mice. This suggests lingual tissues may serve as a new peripheral specimen for surrogate markers of AD, whose discovery holds potential for the development of non-invasive diagnostic tools for AD.

ACKNOWLEDGEMENTS

This work was supported by a research grant from Seoul National University (800-20220546 to O.K.), by National Research Foundation of Korea (NRF) grants funded by the Korean Government (the Ministry of Science and ICT, RS-2023-00208193 and NRF-2022M3A9F3094559 to Y.T.J., NRF-2020R1A4A3078962 and NRF-2020R1C1C1008033 to O.K.), and by a Korean Fund for Regenerative Medicine (KFRM) grant funded by the Korea government (the Ministry of Science and ICT, the Ministry of Health & Welfare, 21C0712L1 to Y.T.J.). We would like to express our gratitude to the Institute of Biomedical Science & Food Safety, CJ-Korea University Food Safety Hall (Seoul, Republic of Korea) for providing technical support associated for this study.

REFERENCES

1. Gaddey HL (2017) Oral manifestations of systemic disease. Gen Dent 65:23-29.
2. Jang JH, Kwon O, Moon SJ, Jeong YT (2021) Recent advances in understanding peripheral taste decoding I: 2010 to 2020. Endocrinol Metab (Seoul) 36:469-477.
3. Yee KK, Li Y, Redding KM, Iwatsuki K, Margolskee RF, Jiang P (2013) Lgr5-EGFP marks taste bud stem/progenitor cells in

posterior tongue. Stem Cells 31:992-1000.
4. Stone LM, Finger TE, Tam PP, Tan SS (1995) Taste receptor cells arise from local epithelium, not neurogenic ectoderm. Proc Natl Acad Sci U S A 92:1916-1920.
5. Roper S (1983) Regenerative impulses in taste cells. Science 220:1311-1312.
6. Lee H, Macpherson LJ, Parada CA, Zuker CS, Ryba NJP (2017) Rewiring the taste system. Nature 548:330-333.
7. Donoso JA, Zapata P (1976) Effects of deneravation and decentralization upon taste buds. Experientia 32:591-592.
8. Adpaikar AA, Lee JM, Lee DJ, Cho HY, Ohshima H, Moon SJ, Jung HS (2023) Epithelial plasticity enhances regeneration of committed taste receptor cells following nerve injury. Exp Mol Med 55:171-182.
9. Wood RM, Garcia Z, Daniels N, Landon SM, Humayun S, Lee HG, Macpherson LJ (2020) Selective peripheral taste dysfunction in APP/PS1 mutant transgenic mice. J Alzheimers Dis 76:613-621.
10. Hassan R, Rabea AA, Ragae A, Sabry D (2020) The prospective role of mesenchymal stem cells exosomes on circumvallate taste buds in induced Alzheimer's disease of ovariectomized albino rats: (light and transmission electron microscopic study). Arch Oral Biol 110:104596.
11. Knopman DS, Amieva H, Petersen RC, Chételat G, Holtzman DM, Hyman BT, Nixon RA, Jones DT (2021) Alzheimer disease. Nat Rev Dis Primers 7:33.
12. Puig KL, Combs CK (2013) Expression and function of APP and its metabolites outside the central nervous system. Exp Gerontol 48:608-611.
13. Kim DK, Park J, Han D, Yang J, Kim A, Woo J, Kim Y, Mook-Jung I (2018) Molecular and functional signatures in a novel Alzheimer's disease mouse model assessed by quantitative proteomics. Mol Neurodegener 13:2.
14. Aho L, Pikkarainen M, Hiltunen M, Leinonen V, Alafuzoff I (2010) Immunohistochemical visualization of amyloid-beta protein precursor and amyloid-beta in extra- and intracellular compartments in the human brain. J Alzheimers Dis 20:1015-1028.
15. Luna-Viramontes NI, Campa-Córdoba BB, Ontiveros-Torres MÁ, Harrington CR, Villanueva-Fierro I, Guadarrama-Ortíz P, Garcés-Ramírez L, de la Cruz F, Hernandes-Alejandro M, Martínez-Robles S, González-Ballesteros E, Pacheco-Herrero M, Luna-Muñoz J (2020) PHF-Core tau as the potential initiating event for tau pathology in Alzheimer's disease. Front Cell Neurosci 14:247.
16. Moloney CM, Lowe VJ, Murray ME (2021) Visualization of neurofibrillary tangle maturity in Alzheimer's disease: a clinicopathologic perspective for biomarker research. Alzheimers Dement 17:1554-1574.
17. Li D, Cho YK (2020) High specificity of widely used phospho-tau antibodies validated using a quantitative whole-cell based assay. J Neurochem 152:122-135.
18. Petry FR, Pelletier J, Bretteville A, Morin F, Calon F, Hébert SS, Whittington RA, Planel E (2014) Specificity of anti-tau antibodies when analyzing mice models of Alzheimer's disease: problems and solutions. PLoS One 9:e94251.
19. Dugger BN, Whiteside CM, Maarouf CL, Walker DG, Beach TG, Sue LI, Garcia A, Dunckley T, Meechoovet B, Reiman EM, Roher AE (2016) The presence of select tau species in human peripheral tissues and their relation to Alzheimer's disease. J Alzheimers Dis 54:1249.
20. Gu Y, Oyama F, Ihara Y (1996) Tau is widely expressed in rat tissues. J Neurochem 67:1235-1244.
21. Uhlén M, Fagerberg L, Hallström BM, Lindskog C, Oksvold P, Mardinoglu A, Sivertsson Å, Kampf C, Sjöstedt E, Asplund A, Olsson I, Edlund K, Lundberg E, Navani S, Szigyarto CA, Odeberg J, Djureinovic D, Takanen JO, Hober S, Alm T, Edqvist PH, Berling H, Tegel H, Mulder J, Rockberg J, Nilsson P, Schwenk JM, Hamsten M, von Feilitzen K, Forsberg M, Persson L, Johansson F, Zwahlen M, von Heijne G, Nielsen J, Pontén F (2015) Proteomics. Tissue-based map of the human proteome. Science 347:1260419.
22. Blake JA, Baldarelli R, Kadin JA, Richardson JE, Smith CL, Bult CJ; Mouse Genome Database Group (2021) Mouse genome database (MGD): knowledgebase for mouse-human comparative biology. Nucleic Acids Res 49(D1):D981-D987.
23. Wang Y, Mandelkow E (2016) Tau in physiology and pathology. Nat Rev Neurosci 17:5-21.
24. Braak H, Braak E (1991) Neuropathological stageing of Alzheimer-related changes. Acta Neuropathol 82:239-259.
25. Pearson RC (1996) Cortical connections and the pathology of Alzheimer's disease. Neurodegeneration 5:429-434.
26. Kanaan NM, Grabinski T (2021) Neuronal and glial distribution of tau protein in the adult rat and monkey. Front Mol Neurosci 14:607303.
27. Uemura N, Uemura MT, Luk KC, Lee VM, Trojanowski JQ (2020) Cell-to-cell transmission of tau and α-synuclein. Trends Mol Med 26:936-952.
28. Narukawa M, Takahashi S, Saito T, Saido TC, Misaka T (2020) Analysis of taste sensitivities in app knock-in mouse model of Alzheimer's disease. J Alzheimers Dis 76:997-1004.
29. Hamamichi R, Asano-Miyoshi M, Emori Y (2006) Taste bud contains both short-lived and long-lived cell populations. Neuroscience 141:2129-2138.

30. Perea-Martinez I, Nagai T, Chaudhari N (2013) Functional cell types in taste buds have distinct longevities. PLoS One 8:e53399.
31. Bermejo-Pareja F, Antequera D, Vargas T, Molina JA, Carro E (2010) Saliva levels of Abeta1-42 as potential biomarker of Alzheimer's disease: a pilot study. BMC Neurol 10:108.
32. Lee M, Guo JP, Kennedy K, McGeer EG, McGeer PL (2017) A method for diagnosing Alzheimer's disease based on salivary amyloid-β protein 42 levels. J Alzheimers Dis 55:1175-1182.
33. Tvarijonaviciute A, Zamora C, Ceron JJ, Bravo-Cantero AF, Pardo-Marin L, Valverde S, Lopez-Jornet P (2020) Salivary biomarkers in Alzheimer's disease. Clin Oral Investig 24:3437-3444.
34. Shi M, Sui YT, Peskind ER, Li G, Hwang H, Devic I, Ginghina C, Edgar JS, Pan C, Goodlett DR, Furay AR, Gonzalez-Cuyar LF, Zhang J (2011) Salivary tau species are potential biomarkers of Alzheimer's disease. J Alzheimers Dis 27:299-305.
35. Ashton NJ, Ide M, Schöll M, Blennow K, Lovestone S, Hye A, Zetterberg H (2018) No association of salivary total tau concentration with Alzheimer's disease. Neurobiol Aging 70:125-127.
36. Pekeles H, Qureshi HY, Paudel HK, Schipper HM, Gornistky M, Chertkow H (2018) Development and validation of a salivary tau biomarker in Alzheimer's disease. Alzheimers Dement (Amst) 11:53-60.
37. Hattori H, Matsumoto M, Iwai K, Tsuchiya H, Miyauchi E, Takasaki M, Kamino K, Munehira J, Kimura Y, Kawanishi K, Hoshino T, Murai H, Ogata H, Maruyama H, Yoshida H (2002) The tau protein of oral epithelium increases in Alzheimer's disease. J Gerontol A Biol Sci Med Sci 57:M64-M70.
38. Arredondo LF, Aranda-Romo S, Rodríguez-Leyva I, Chi-Ahumada E, Saikaly SK, Portales-Pérez DP, González-Amaro R, Salgado-Bustamante M, Enriquez-Macias L, Eng W, Norman RA, Jimenez-Capdeville ME (2017) Tau protein in oral mucosa and cognitive state: a cross-sectional study. Front Neurol 8:554.
39. Foidl BM, Humpel C (2020) Can mouse models mimic sporadic Alzheimer's disease? Neural Regen Res 15:401-406.
40. Lim S, Haque MM, Su D, Kim D, Lee JS, Chang YT, Kim YK (2017) Development of a BODIPY-based fluorescent probe for imaging pathological tau aggregates in live cells. Chem Commun (Camb) 53:1607-1610.